Vol 10 No 2, February 2001
1009-1963/2001/10(02)/0134-05

Chinese Physics

© 2001 Chin. Phys. Soc.
and IOP Publishing Ltd

STUDY OF THE CORRELATION BETWEEN POWER DEPOSITION OF THE LOWER HYBRID WAVES AND THE HARD X-RAY RADIATION ON HT-7 TOKAMAK

Shi Yue-jiang(石跃江), Wan Bao-nian(万宝年),
Ling Bi-li(凌必利), and Ding Bo-jiang(丁伯江)
Institute of Plasma Physics, Chinese Academy of Sciences, Hefei 230031, *China*

(Received 28 May 2000; revised manuscript received 11 July 2000)

A seven-channel NaI(Tl) detector array installed on an HT-7 superconducting tokamak has been used to detect the hard X-ray ($E_{h\nu}$ >20 keV) emitted from the plasma. The physical mechanism of the lower hybrid waves propagating and absorbed in the plasma is investigated by the measurement of the hard X-ray radial profile at different discharge parameters.

Keywords: hard X-ray, low hybrid waves, NaI (Tl) detector
PACC: 5225N, 5250G, 5255F

I. INTRODUCTION

Steady-state operation is the precondition to realize a commercial fusion reactor. Due to the limited volt-seconds of an ohmic heating (OH) transformer, a tokamak operating with an inductively generated plasma current is just a pulse device. In particular, it is essential to develop non-inductive methods for the tokamak power reactor. Fisch[1] put forward the theory of lower hybrid current drive (LHCD) in 1978. In many tokamaks, including HT-7, the technique of LHCD[2] was developed, and LHCD has been demonstrated to be an effective non-inductive current drive method and a powerful tool to control plasma current profile. In JT-60U, it is successful in applying LHCD for the sustainment of reversed magnetic shear configuration and the control of the position of the internal transport barrier for several seconds.[3] It is considered to be the most promising candidate for an advanced steady-state operation of a tokamak fusion reactor.[4] In the HT-7 tokamak, improved confinement during LHCD has been observed.[5] Evidence shows that confinement improvement is impacted by low hybrid wave (LHW) power deposition, i.e., the current profile. Since the mechanism is not fully understood, it is of great importance to investigate the power deposition of LHW.

During LHCD, a non-Maxwellian current carrying a tail of energetic electrons is created by LHW. The electron tail is formed through Landau damping of the LHWs. This high-energy tail emits a continuum bremsstrahlung radiation due to collisions between the tail electrons and the bulk plasma ions and electrons (the electron–ion bremsstrahlung is dominant[6]). Much important information about the high-energy electrons and the physical mechanism of LHW propagation and absorption in plasma can be obtained from the hard X-ray measurement. For many tokamaks,[6–8] high-energy electron distribution function has been gained and the accessibility condition has been verified by hard X-ray measurement.

A seven-channel NaI(Tl) detector array installed on a HT-7 tokamak has been used to measure the hard X-ray emission during LHCD. The correlation between power deposition of LHW and hard X-ray radiation has been investigated. The experimental results indicate that the hard X-ray radial profile has a close relation with the power spectrum of LHW and the parameters of plasma.

II. EXPERIMENTAL DEVICES AND DIAGNOSTICS

HT-7 is a superconducting tokamak with a major radius R_0=122 cm, a minor radius a=30 cm and the magnetic field $B_t \leq$2.5 T. Its LHW power source consists of twelve klystrons, each generating a maximum power of 100 kW at a frequency of 2.45 GHz. The maximum power of the whole RF system is 1.2 MW.

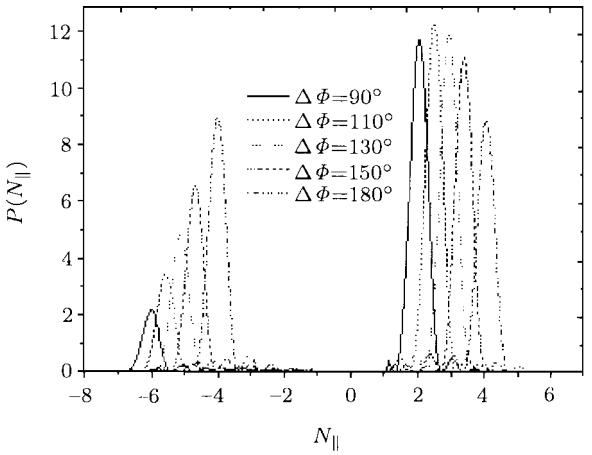


Fig.1. The Brambilla $N_{\|}$ power spectrum for the HT-7 waveguide array.

A grill coupler composed of 2×12 subwaveguides is used to launch the waves from the twelve klystrons. The waveguide phasing between the adjacent subwaveguides can be set at any desired value. Through adjusting the waveguide phasing ($\Delta\Phi$) between the adjacent subwaveguides, it is flexibly in control of the launched power spectrum, hence achieving the optional coupling between the wave and the plasma. The theoretical Brambilla $N_{\|}$ power spectrum for the HT-7 waveguide array is shown in Fig.1.

Figure 2 shows a schematic diagram of the seven-channel NaI (Tl) detector array on the HT-7 superconducting tokamak. The array observes the hard X-ray emitted perpendicular to the magnetic axis through a horizontal window. The seven detectors are arranged parallel from bottom to top. Each detector of the array views the emission from a particular choral (radial) position in the plasma, ranging from −21 to 21 cm. To prevent stray hard X-rays emitted from the vacuum vessel and plasma limiter, the entire array is placed inside a lead shield approximately 15 cm thick. These viewing lines are tightly collimated with a diameter of 1 cm so that only the plasma column is observed. The vacuum window is made of 0.5 mm thick beryllium that will block off the photons with energies less than 20 keV. The stopping efficiency of 40×40 mm NaI crystals is almost 100% to the photons of 20–500 keV. The detectors are calibrated by the radioactive isotope ^{152}Eu.

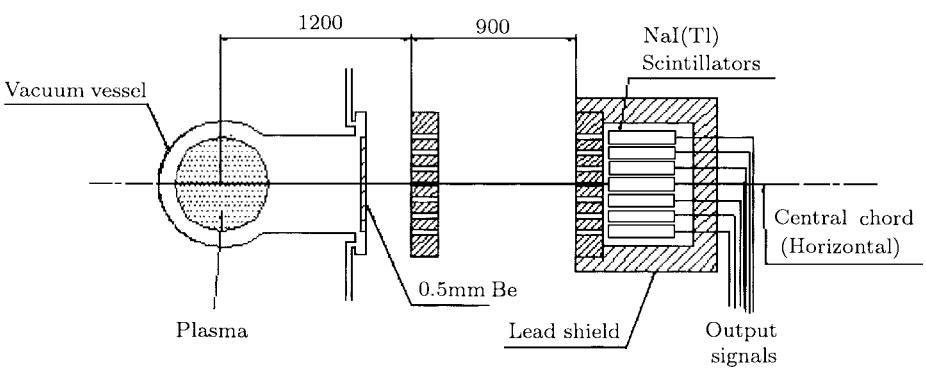


Fig.2. Schematic diagram of the NaI(Tl) scintillator array.

Ⅲ. EXPERIMENTAL RESULTS AND DISCUSSION

To drive the current, the LHW accessibility requires $N_{\|} > N_{\|\mathrm{acc}}$. The parallel refractive index of the wave ($N_{\|}$) depended on the antenna. $N_{\|\mathrm{acc}}$ is determined by the cold plasma lower hybrid theory[9]

$$N_{\|\mathrm{acc}} = \frac{\omega_{\mathrm{pe}}}{\omega_{\mathrm{ce}}} + \sqrt{1 + \left(\frac{\omega_{\mathrm{pe}}}{\omega_{\mathrm{ce}}}\right)^2 - \left(\frac{\omega_{\mathrm{pi}}}{\omega}\right)^2},$$

where ω is the wave frequency, ω_{pe} the local plasma electron frequency, ω_{pi} the local plasma ion frequency and ω_{ce} the electron cyclotron frequency. The ω_{pi} can be neglected for $\omega_{\mathrm{pi}} << \omega$. Because ω_{pe} and ω_{ce} are associated with the toroidal magnetic field (B_{t}) and plasma electron density (N_{e}), respectively, B_{t} and N_{e} are two important plasma parameters to determine the accessibility condition.

Figure 3 shows the waveforms of an LHCD discharge on HT-7. The LHW (320 kW) is injected at 250 ms and turns off at 550 ms. The line averaged

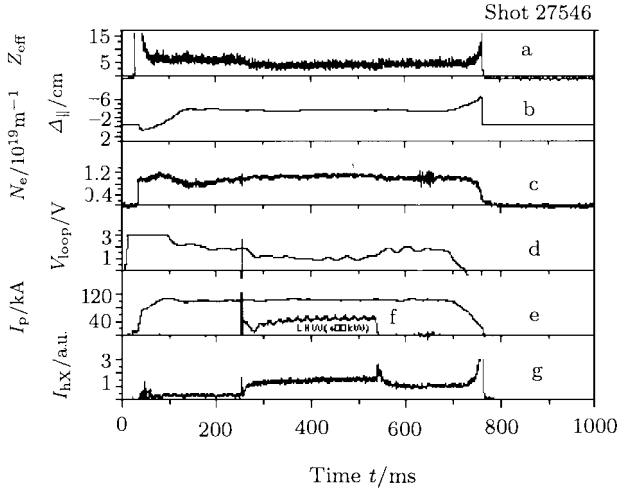


Fig.3. Waveforms of LHCD discharge on HT-7: (a) effective charges $Z_{\rm eff}$; (b) horizontal displacement $\Delta_{\parallel}$; (c) line average density $N_{\rm e}$; (d) loop voltage $V_{\rm loop}$; (e) plasma current $I_{\rm p}$; (f) power of LHW; (g) hard X-ray intensity $I_{\rm HX}$.

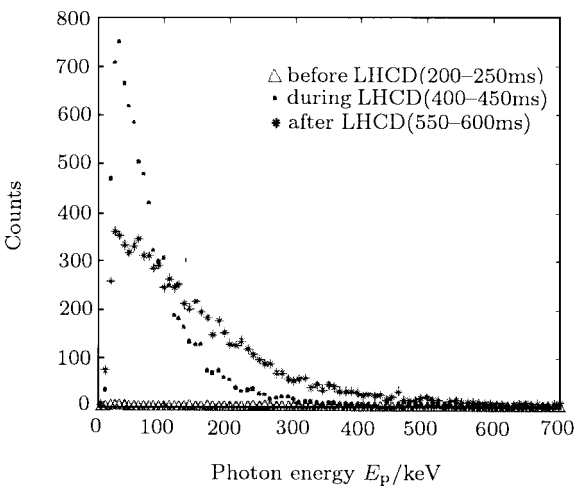


Fig.4. The hard X-ray spectrum of the central chord.

electron density is $1\times10^{13}\,{\rm cm}^{-3}$ and kept almost constant. During the injection of LHW, the horizontal displacement of plasma and $Z_{\rm eff}$ are steady, but the hard X-ray intensity increases remarkably. From the hard X-ray spectrum (Fig.4), we can see that the hard X-ray emission is very small before LHCD, compared to the emission during LHCD. The energy of most photons is less than 150 keV, which suggests the high-energy tail is not the runaway electron tail. The increase of hard X-ray intensity indicates the LHW drives out high-energy electrons that carry plasma current and make a drop of loop voltage. There is a jump in hard X-ray emission when the LHW turns off. The reason is that the high-energy electrons are restricted in the range of resonance by the wave during LHCD. These tail electrons are accelerated to a higher energy and will run away due to the force of electric field after the LHW turns off.

With the same plasma parameters ($\overline{N}_{\rm e}=1.0\times10^{13}\,{\rm cm}^{-3}$, $B_{\rm t}=1.9\,{\rm T}$ and the power of LHW $P_{\rm LH}=320\,{\rm kW}$), Fig.5 shows the hard X-ray radial intensity distribution at different $\Delta\Phi$. When the LHW has a smaller $\Delta\Phi$ ($N_{\parallel{\rm peak}}=2.45$, the LHW still satisfies the accessibility condition for the plasma central region), the hard X-ray photons are mainly emitted from the inner half ($r/a<1/2$) of the plasma column. This indicates that the LHW deposits most energy in this part ($r/a<1/2$). On the other hand, the hard X-ray radial profile becomes broader when the LHW has larger $\Delta\Phi$ ($N_{\parallel{\rm peak}}=3.5$). This means that a greater

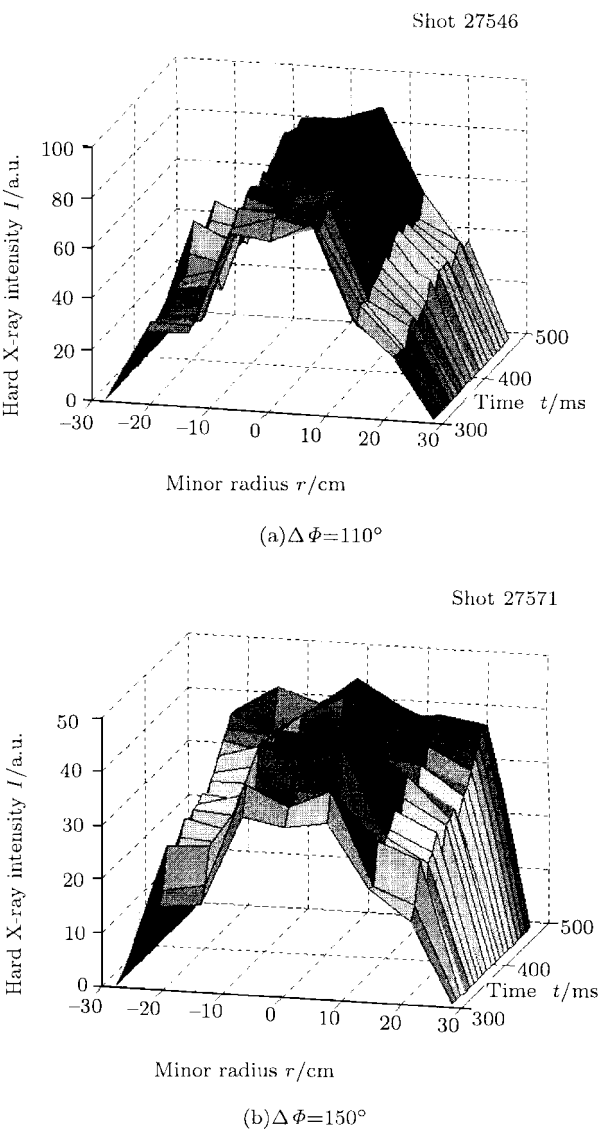


Fig.5. The hard X-ray radial profile at different waveguide phasing.

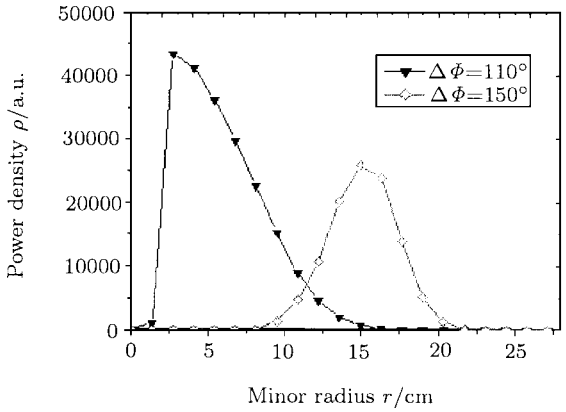
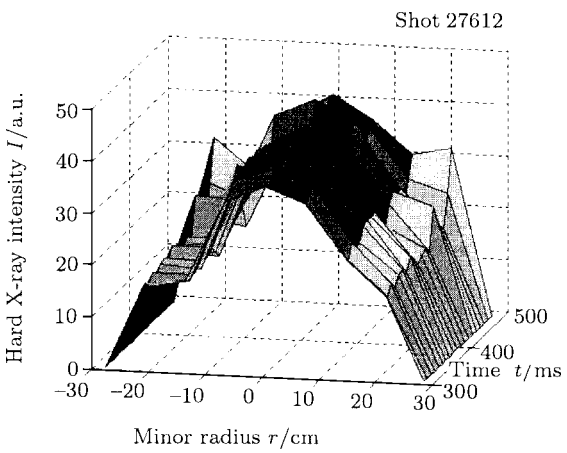
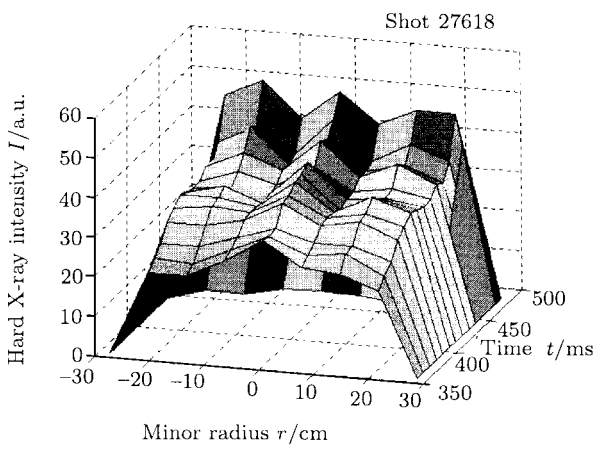


Fig.6. Predicted power deposition profile of LHW calculated by ray-tracing code.

fraction of the LHW power is being damped in the outside of the plasma column. The LHW with a larger $\Delta\Phi$ has a smaller parallel phase velocity, and there will be enough electrons that satisfy the resonance condition in the peripheral region of plasma, even if the electron density is quite low, so the LHW is intensely absorbed by the plasma in the periphery. In contrast, the LHW with a smaller $\Delta\Phi$ has a larger parallel phase velocity and will be weakly absorbed in the periphery of the plasma column. Thus, it can propagate into the plasma core where the electron density is higher, compared to that of periphery, and more electrons can satisfy the resonance condition. Moreover, the up shift of $N_{\|}$ during the waves propagating into the interior is beneficial to the absorption of waves as well. Fig.6 shows the numerical simulation results by ray-tracing code.[10] It can be seen that the experimental results agree with the theoretical calculations in general.

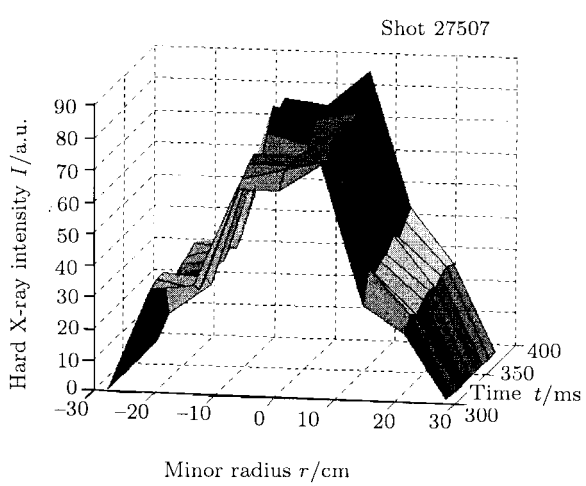


(a) N_{co}=0.9×10^{19}m^{-3}

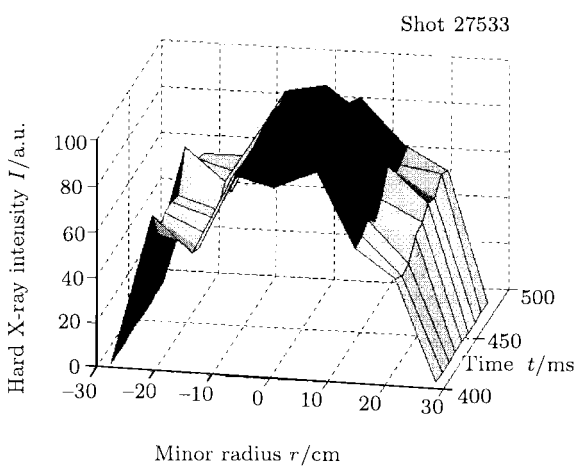


(b) N_{co}=3.1 × 10^{19}m^{-3}

A. The hard X-ray radial profile at different electron densities.



(a) B_t=2.1T



(b) B_t=1.6T

B. The hard X-ray radial profile at different toroidal magnetic field

Fig.7. The hard X-ray radial profile at different plasma parameters. The other main parameters are:$\Delta\Phi$=110°, I_p=110 kA, P_{LH}=320 kW.

Figure 7 shows the hard X-ray radial profile at different plasma electron density (N_e) and toroidal magnetic field (B_t). The hard X-ray radial profile is highly peaked at lower plasma density or higher toroidal magnetic field. On the other hand, the hard X-ray radial profile becomes flatter at higher plasma density or lower toroidal magnetic field. The experimental results agree with the condition of accessibility. Smaller $N_{\|acc}$ can be obtained at lower N_e or higher B_t, hence more LHW beams can propagate into the plasma interior and interact with the plasma, so more high-energy electrons will be driven out in the core of plasma and a peaked hard X-ray radial profile is formed. When N_e increases or B_t decreases, $N_{\|acc}$ will increase accordingly, so the LHW with low $N_{\|}$ cannot propagate into the core of the plasma and mainly interacts with the plasma in the periphery where both N_e and B_t are smaller than those at the centre. Therefore, more high-energy photons will be emitted from the peripheral region of the plasma.

IV. CONCLUSIONS

The correlation between the power deposition of the LHW and hard X-ray radiation has been investigated. The hard X-ray radial profile can directly reflect the power deposition of the LHW. The hard X-ray radial profile has a close relation with the power spectrum of LHW and the plasma electron density and toroidal magnetic field. The main experimental results can be summarized as follows.

The wave with a smaller $\Delta\Phi$ will deposit its energy primarily within the inner region of the plasma column, while the wave with a larger $\Delta\Phi$ will deposit its energy mainly in the peripheral region of the plasma.

The hard X-ray radial profile peaks at a lower plasma density or higher toroidal magnetic field.

The hard X-ray profile will become broadened at a higher plasma density or lower toroidal magnetic field.

This work demonstrates that the hard X-ray detector array is a good monitor for the LHW power deposition. Further work will be done to investigate the correlation of confinement with power deposition of LHW and current profile.

ACKNOWLEDGMENTS

We are grateful to the HT-7 tokamak group and the LHCD staff for their assistance and collaboration.

References

[1] Fisch N J 1978 *Phys. Rev. Lett.* **41** 873

[2] Kuang G, LHCD Group of ASIPP, in *Controlled Fusion and Plasma Physics* (1997 *Proc. 24th Eur. Conf. Berchtesgaden*), A **21**, Part I, 1997 European Physical Society, Geneva p 457

[3] Ide S, Fujita T, Natio O and Seki M 1996 *Plasma Phys. Control Fusion* **38** 1645

[4] Taylor T S 1997 *Plasma Phys. Control Fusion* **39** B47

[5] Kuang G, Liu Y and Shan J *et al.* 1999 *Nucl. Fusion* **39** 1769

[6] Geoler S V, Steven J and Bernabei S *et al.* 1985 *Nucl. Fusion* **25** 1515

[7] Texter S, Knowlton S, Porkolab M and Takase Y 1986 *Nucl. Fusion* **26** 1279

[8] Ogura K, Tanaka H, Ide S *et al.* 1991 *Nucl. Fusion* **31** 1015

[9] Karney C F F and Fisch N J 1979 *Phys. Fluids* **22** 1817

[10] Bonoli P T and Englade R C 1986 *Phys. Fluids* **29** 2937